HHS Public Access

Author manuscript

J Neuropathol Exp Neurol. Author manuscript; available in PMC 2011 April 01.

Published in final edited form as:

J Neuropathol Exp Neurol. 2010 April ; 69(4): 356–371. doi:10.1097/NEN.0b013e3181d53d98.

Paxillin and Hydrogen Peroxide-Inducible-Clone 5 (Hic-5) Expression and Distribution in Control and Alzheimer Disease Hippocampus

John Caltagarone, PhD, **Ronald L. Hamilton, MD**, **Geoffrey Murdoch, MD**, **Zheng Jing, PhD**, **Donald B. DeFranco, PhD**, and **Robert Bowser, PhD**

From the Departments of Pathology (JC, RLH, GM, RB), and Center for Neuroscience (ZJ), and Pharmacology (JC, DBD), and Pittsburgh Institute for Neurodegeneration (DBD, RB), University of Pittsburgh, Pennsylvania.

Abstract

Hydrogen peroxide-inducible-clone 5 (Hic-5) and paxillin are members of the group III LIM domain protein family that localize to both cell nuclei and focal adhesions and link integrin-mediated signaling to the actin cytoskeleton. Prior in vitro studies have implicated paxillin in β-amyloid-induced cell death but little is known about the expression and function of Hic-5 and paxillin in the brain. We performed a blinded retrospective cross-sectional study of Hic-5 and paxillin expression in the hippocampus of Alzheimer disease (AD) and control subjects using immunohistochemistry and laser scanning confocal microscopy. The analysis included assessment of the expression of phosphorylated isoforms of paxillin that reflect activation of distinct signaling pathways. We found changes in the subcellular distribution of Hic-5, paxillin and specific phosphorylated isoforms of paxillin in the AD brains. Hic-5 and phosphorylated isoforms of paxillin colocalized with neurofibrillary tangles. Paxillin was predominantly found in reactive astrocytes in the AD hippocampi and activated paxillin was also detected in granulovacuolar bodies in AD. These data indicate that these important scaffolding proteins that link various intracellular signaling pathways to the extracellular matrix are modified and have altered subcellular distribution in AD.

Keywords

Alzheimer disease; Amyloid plaque; Focal adhesions; Granulovacuolar degeneration; Hippocampus; Neurofibrillary tangles

Send correspondence and reprint requests to: Robert Bowser, PhD, Department of Pathology, University of Pittsburgh School of Medicine, BST S-420, 200 Lothrop St., Pittsburgh, PA 15261. Phone: 412-383-7819; FAX: 412-648-1916; Bowserrp@upmc.edu.

INTRODUCTION

The participation of focal adhesion proteins in the pathogenesis of Alzheimer disease (AD) has been postulated based upon integrin-mediated interactions with β-amyloid in vitro (1–5). β-amyloid-induced activation of integrins in AD might trigger downstream signaling events that are linked to focal adhesion complexes thereby differentially affecting cell functions and survival. Therefore, an analysis of focal adhesion proteins that link integrin activation to downstream signaling cascades may provide insight into cellular responses in AD.

Focal adhesions are macromolecular protein complexes that link integrin-mediated signaling to the actin cytoskeleton (6–9). Upon cell adhesion, integrins utilize both structural and signaling cell adhesion molecules to impact cellular motility and viability (7–10). During the initial stage of cell adhesion to the extracellular matrix (ECM), numerous proteins are required for focal adhesion assembly; the activity of each of these may be regulated by specific post-translational modifications such as phosphorylation (7–9, 11–14). For example, integrin activation leads to the phosphorylation and sequestration of LIM domain containing proteins, such as paxillin that may create an intracellular scaffold for many interacting cytoskeleton signaling proteins (6, 15, 16). Paxillin and the closely related protein Hic-5 are members of the group III LIM domain family that contain 7 zinc fingers, at least 4 N-terminus leucine-rich motifs termed LD motifs, and numerous sites modified by phosphorylation (6, 15–20). Hic-5 and paxillin share many interacting partners. Because of the close relatedness of their LIM domains, they are believed to act competitively or antagonistically in many signal transduction pathways (15, 17, 21–24). Paxillin is phosphorylated on tyrosine amino acid residues 31 and 118 (pY31 and pY118) upon the initial activation of ECM-integrin signaling and the formation of intracellular focal adhesion sites (5, 15, 25–28). Specific phosphorylation of paxillin is required for activation of distinct downstream signaling pathways (26, 27, 29–31). The integration of a variety of signaling cascades is further influenced by the ability of some focal adhesion proteins to regulate gene expression (10, 16). Indeed, both Hic-5 and paxillin localize within both cytoplasmic focal adhesions and the nucleus (10). The ability to act both in the nucleus and focal adhesions suggests that intracellular trafficking impacts their biological effects. Hic-5 contains 2 nuclear export signal sequences but oxidative injury induces Hic-5 nuclear import in cultured fibroblasts (18). Hic-5 has also been shown to be both a positive and negative co-regulator of gene expression (32–38).

Hic-5 and paxillin are expressed in numerous regions of the rat brain including cerebellum, striatum, prefrontal cortex, hippocampus, hypothalamus, thalamus, and spinal cord (39). Although little is known about the specific roles of paxillin and Hic-5 in regulating focal adhesion signaling and gene expression within brain, non-genomic roles for both paxillin and Hic-5 in brain have been described. For example, paxillin is rapidly phosphorylated in the presence of fibrillar β-amyloid and colocalizes with hyperphosphorylated tau (pTau) in cultured neurons (1). This altered subcellular distribution increases focal adhesion turnover and altered cell mobility and plasticity associated with a loss of synaptic integrity (1, 40). Hic-5 decreases cell surface levels of dopamine transporter (DAT) in rat midbrain neuronal cultures and negatively affects dopamine uptake (39). A direct interaction between Hic-5 and DAT may be responsible for this effect. These reports suggest biologic functions of

Hic-5 and paxillin in the brain but a detailed analysis of paxillin and Hic-5 expression and distribution in control and AD brains has not been performed.

In view of the in vitro association between paxillin and β-amyloid-induced toxicity and Hic-5 response to oxidative stress and since the generation of amyloid plaques and neurofibrillary tangles (NFTs), the main hallmarks of AD, is influenced by reactive oxygen species and altered cell signaling pathways (41–43), we hypothesized that these associations may be involved in AD pathogenesis. Therefore, we performed a blinded retrospective analysis of the expression and subcellular distribution of Hic-5 and paxillin in hippocampi of 10 AD and 5 age-matched non-neurologic disease control subjects using immunohistochemistry (IHC). Laser scanning confocal microscopy was used to colocalize Hic-5, paxillin and phosphorylated isoforms of paxillin with the pathological hallmarks of AD. Our results provide novel insights regarding the expression and distribution of Hic-5 and paxillin in control and AD brain and of the phosphorylated isoforms of paxillin that are altered in AD.

MATERIALS AND METHODS

Human Brain Tissue

The Committee for Oversight of Research Involving the Dead at the University of Pittsburgh School of Medicine approved the use of human tissue from the University of Pittsburgh Tissue Bank. A blinded retrospective cross-sectional study involving age-matched postmortem brains was performed using 5 cases with no clinical history of a neurodegenerative disease or AD pathology, 5 cases with pathologically defined “early-stage” AD, and 5 cases pathologically defined “late-stage” AD (Table 1). All cases were categorized according to Braak staging and grouped for analysis into 3 categories: control (Braak stage 0–I); Braak stage II-III; and Braak stage V-VI. The study consisted of 10 patients who were clinically diagnosed as having “probable AD” using the National Institute of Neurological and Communication Disorder and Stroke/Alzheimer’s Disease and Related Disorders Association criteria with subsequent postmortem neuropathologic confirmation of AD using the Consortium to Establish a Registry for AD, Braak criteria, and the National Institute of Aging-Reagan Institute criteria (41, 44–47). Bielschowsky impregnations were performed on all cases.

Western Blot

Tissue extracts were prepared essentially as previously described (48). Briefly, fresh-frozen human hippocampi from control and AD subjects were homogenized in 20% w/v of ice-cold Tris-Triton X-100 (TX-100) buffer with protease (Sigma, St. Louis, MO) and phosphatase (Calbiochem, La Jolla, CA) inhibitors. The homogenate was centrifuged at 500 × *g* to remove debris and then centrifuged at 100,000 × *g* at 4°C. The supernatant was saved containing the TX-100-soluble fraction. The pellet containing the TX-100-insoluble fraction was resuspended in TX-100 buffer. The protein concentration for TX-100-soluble and -insoluble fractions was quantitated using the BCA Protein Assay Kit (Pierce). Fifty μg protein/lane for each subject was separated on a 10% SDS-PAGE and transferred to nitrocellulose membrane. Nonspecific antigens were blocked with 5% dry milk for 1 hour at

room temperature and incubated overnight at 4°C with primary antibodies. Immunoblots were then incubated with horseradish peroxidase-conjugated secondary antibodies (Chemicon International, Temecula, CA) and developed using ECL (PerkinElmer Life Sciences, Boston, MA). Protein levels were quantified after scanning the appropriate molecular weight on the film using NIH Image 1.63. Each lane was normalized to actin and the most intense band was arbitrarily set to 100%. Antibodies used for Western blot and IHC are listed in Table 2.

Immunohistochemistry and Laser Scanning Confocal Microscopy

Tissue was immersion-fixed in 10% buffered formalin and embedded in paraffin. Hippocampal tissue sections, 8 μm thick, were heated to 60°C for 1 hour prior to deparaffinization via 100% xylene and re-hydration. Endogenous peroxidase activity in the tissue was blocked with 0.3% H_2O_2 for 30 minutes. To expose antigenic epitopes, sections were steamed for 20 minutes in target retrieval solution (DAKO, Carpinteria, CA). To reduce nonspecific primary antibody labeling for endogenous biotin, biotin receptors, and avidin binding sites in tissue, the avidin/biotin blocking kit was used according to company specifications (Vector Laboratories, Burlingame, CA). To block general nonspecific tissue antibody binding sites in tissue, SuperBlock (ScyTek Laboratories, Logan, UT) was added to tissue for 10 minutes. A no-primary antibody control slide was used to determine nonspecific immunoreactivity associated with the secondary antibodies. Tissue slides across all cases for each antibody were performed simultaneously to avoid day-to-day variability and were also not counterstained to permit accurate interpretation of the staining patterns. Commercial blocking peptides for phosphorylated Y118 (pY118) and pS126 paxillin were used to demonstrate specificity of the immunostaining. For the blocking peptides, brain tissue was incubated with antibody and 100-fold molar excess of either specific blocking peptides or nonspecific blocking peptides. Immunoreactivity on the tissue slides were visualized with Nova-Red chromogen (Vector Laboratories), dehydrated and mounted with Permount (Fisher, Pittsburgh, PA).

Confocal microscopy was performed as previously described except secondary antibodies were conjugated to Alexa Fluor-488 and –568. Triple labeling was performed by incubation with the far-red fluorescent nucleic stain TO-PRO-3 (Invitrogen, Carlsbad, CA). Pyramidal neurons in human brain are known to contain elevated levels of lipofuscin granules typically localized within the soma, which exhibit significant autofluorescence at longer wavelengths. Therefore, to minimize the contribution of autofluorescence to laser scanning confocal microscopy signals, secondary antibodies conjugated to Alexa Fluor –488 were used for Hic-5 or paxillin while Alexa Fluor –568 were used for colocalization with well-characterized markers for AD pathology.

Immunoprecipitation

Fresh frozen hippocampi from control and AD subjects were homogenized in 5 volumes of cold lysis buffer (50 mM Tris HCL pH 7.4, 150 mM NaCl, 1% Triton X-100, 1% sodium deoxycholate-stage, 0.1% SDS, protease (Sigma) and phosphatase (Calbiochem) inhibitors in a glass-Teflon homogenizer (500 rpm, 10 strokes). 100 μl of total homogenate from control and AD subjects were pre-incubated with 4 μl primary antibodies for 2 hours. The

tissue lysate was then mixed with Protein G Magnetic Microbeads for 30 minutes. To activate the μMACS columns (Miltenyi Biotec, Auburn, CA), 200 μl of lysis buffer was added before the immunoprecipitates were captured using the magnetic field. After the tissue lysate flowed through the columns, they were washed 4× 200 μl lysate buffer, 1× 200 μl high salt buffer (500 mM NaCl, 1% NP-40, 50 mM Tris HCL pH 8.0, and 1× 200 μl low salt buffer (20 mM Tris HCL pH 7.5). To elute the bound complexes, 20 μl of pre-heated (95°C) 1× sample buffer (200 mM Tris HCL 6.8, 0.2% SDS, 10% glycerol, 0.01% bromphenol blue) was added to the column for 5 minutes. 80 μl of 1× sample buffer was then added and the flow-through was saved. To control for nonspecific binding of protein to μMACS columns, control or AD tissue lysates were combined with Microbeads without prior incubation with primary antibodies and monitored proteins that eluted from the column.

Rank Order and Statistical Analysis

The rank "intensity" order test was used as a non-parametric statistical method (49). The intensity of protein expression was ranked from lowest to highest based on blinded qualitative observations and assigning values of 1 to 15. The rank "intensity" order was then divided into groups based on the unblinded clinical information. The Mann-Whitney (U) test was used when comparing intensity differences in control vs. AD subjects; the Kruskal-Wallis (ANOVA) test was used when comparing control (Braak stage 0-I), Braak stage II-III and Braak stage V-VI subjects (GraphPad Prism 4.0a).

RESULTS

Immunoblot Analysis for Hic-5 and Paxillin

Immunoblot analysis of cell extracts from cultured prostate stromal cells (WPMY-1) and mouse embryonic fibroblast cells (MEF) known to express either Hic-5 (WPMY-1) or paxillin (MEF) were used to demonstrate specificity of each antibody. Small interfering RNA to Hic-5 or genetic ablation of the paxillin gene in cultured cells demonstrated specific immunoreactive bands of the appropriate molecular mass for each antibody (Supplemental Fig. 1). Also included in each gel are the TX-100-soluble (100,000-*g*) and -insoluble tissue extracts prepared from control and AD hippocampus. A non-specific lower molecular weight band was detected by many of the anti-paxillin antibodies but specific bands of the appropriate mass were observed in control and AD brain extracts.

Both TX-100-soluble and -insoluble fractions of control and AD hippocampi revealed a specific Hic-5+ band of the appropriate MW (Fig. 1). Hic-5 levels in the TX-100-soluble fraction trended to decrease ($p < 0.087$) in Braak stage II-II and Braak stage V-VI compared to control subjects (Fig. 1A, C). Hic-5 protein levels in the TX-100-insoluble fraction were significantly decreased ($p < 0.012$) in Braak stage II-II compared to control and Braak stage V-VI AD subjects (Fig. 1B, D). Paxillin was present in the TX-100-soluble fractions in all cases but we did not detect any overall changes in AD compared to controls (data not shown).

Hic-5 and Paxillin Distribution in the Hippocampus

Classical plaques are composed of a heterogeneous population of extracellular Aβ deposits, dystrophic neurites, NFTs, activated astrocytes and microglia (42, 43). Therefore, double-label confocal microscopy with markers specific to plaques (β-amyloid), NFTs (AT8), activated astrocytes (glial fibrillary acidic protein [GFAP]) and microglia (CD68) were used to determine the localization of Hic-5 and paxillin in AD brains. In control and AD hippocampi, Hic-5 immunoreactivity was observed predominately in cell bodies of pyramidal neurons throughout the stratum pyramidale layer (Fig. 2A), in dentate gyrus neurons and round cells of the stratum oriens layer (data not shown). Hic-5 was occasionally detected within pyramidal neuron nuclei in both AD and control hippocampi. Hic-5 immunoreactivity in astrocytes was not observed in controls. By rank order analysis, Hic-5 immunoreactivity was determined to be significantly greater in CA1 pyramidal neurons in AD vs. control subjects (Fig. 2B, C). This observation contradicts in vitro studies in which Hic-5 was found to be predominantly in the nucleus. We also detected Hic-5 in endothelial and smooth muscle cell nuclei of surrounding arteries and large capillaries (data not shown).

By double-label confocal microscopy with markers specific to β-amyloid plaques, NFTs, activated astrocytes and microglia Hic-5 immunofluorescence was observed within pyramidal neuron neurites, cell bodies and nuclei throughout AD hippocampi (Fig. 3). Hic-5+ pyramidal neurons were also adjacent to β-amyloid-containing plaques (Fig. 3a–c); it was also detected in beaded neuritic processes throughout the hippocampi and in a subset of plaques (Fig. 3a, j). A majority of AT8+ NFTs including those adjacent to plaques were Hic-5+ (Fig. 3d–i). Colocalization of Hic-5 in AT8+ NFTs was evident in perinuclear regions or limited to large processes proximal to the cell body (Fig. 3d–i). AT8+ neuropil threads were negative for Hic-5 and it was not observed in extracellular ghost tangles (Fig. 3d–i). Hic-5 was often seen within plaque cores (Fig. 3a–c); it was not localized to GFAP+ astrocytes (not shown) but there was some colocalization with CD68 in microglia (Fig. 3j–l).

By light microscopy, paxillin was predominately located to the outer white matter closest to the lateral ventricle and the stratum lacunosum in control hippocampi (Fig. 4Aa, b). Paxillin was detected in the nucleus and cytoplasm of reactive astrocytes and neuropil within the hilus/CA4 region of all cases and was also present in astrocytes within hippocampal subfields in AD cases (Fig. 4Ac, d). At higher-power magnification, paxillin was observed in focal nuclear granules of CA1 pyramidal neurons in controls; these were present to a lesser degree in AD (Fig. 4Ae, f). By rank order analysis there was a statistically significant increase in paxillin immunoreactivity in AD (Fig. 4B), but this difference did not reach statistical significance when the AD subjects were separately categorized to Braak stages (data not shown). We also detected paxillin in nuclei of choroid plexus cells in control subjects, with loss of nuclear immunostaining in AD (Supplemental Fig. 2). Therefore, paxillin immunoreactivity is elevated in reactive astrocytes and decreased in the nuclei of CA1 pyramidal neurons and choroid plexus cells in AD.

To define cell types expressing paxillin and any association with AD pathology, we performed double-label confocal microscopy. Paxillin was elevated in cells containing numerous processes surrounding and penetrating β-amyloid-containing plaques in AD (Fig. 5a–c). These cells colocalized with GFAP (Fig. 5d–f), consistent with observations by light

microscopy (Fig. 4A). Colocalization of paxillin and GFAP was not evenly distributed and appeared in discrete locations within the glial processes (Fig. 5f). Paxillin was not detected in AT8+ NFTs (Fig. 5g–i).

Distribution of Activated Paxillin in AD

To identify cell types that exhibit activated paxillin (i.e. pY31 and pY118), we performed light and confocal microscopy. In control subjects, pY31 paxillin immunoreactivity was distributed throughout the soma, processes and in nuclei of hippocampal pyramidal neurons (Fig. 6Aa). In AD, pY31 paxillin was observed in the cytoplasm and as punctate structures within the soma, with comparatively lower levels in neuronal nuclei (Fig. 6Ab). pY31 paxillin immunoreactivity was observed in both Hirano bodies and plaques (Fig. 6Ac, d). By confocal microscopy, pY31 paxillin was observed in pyramidal neurons and colocalized with AT8 in soma and neuritic processes (Fig. 6Ba–f). Within plaques, pY31 paxillin was present in both AT8+ and -negative neuritic processes (Fig. 6Bd–f).

Paxillin pY118 immunoreactivity was predominately located in the nuclei of hippocampal pyramidal neurons in control subjects (Fig. 7Aa). In AD, pY118 paxillin immunoreactivity was decreased within nuclei and present in granulovacuolar degeneration (GVD) bodies (Fig. 7Ab). The specificity of the pY118 paxillin immunoreactivity was confirmed using phosphorylated and non-phosphorylated blocking peptides (Fig. 7Ac, d). By confocal microscopy, pY118 paxillin was observed in AT8+ NFTs and plaques but not in neuritic threads (Fig. 7B). Abundant pY118 paxillin was observed within nuclei of neuronal and non-neuronal cells (Fig. 7B).

We next examined phosphorylation of serine residues in paxillin within control and AD brain. Phosphorylation of serine residues is regulated by the JNK pathway and modulates cell migration. Immunoreactivity for paxillin phosphorylated on serine residue 126 (pS126) was detected in the somata and nuclei of neurons throughout the hippocampi of control subjects (Fig. 8A). Within AD hippocampi, pS126 paxillin was detected in structures resembling GVD bodies in the cytoplasm of CA1 pyramidal neurons (Fig. 8Ab). The specificity of the pS126 paxillin antibody was confirmed using phosphorylated and non-phosphorylated blocking peptides (Fig. 8Ac, d). By confocal microscopy, pS126 paxillin was observed in pyramidal neurons and it was colocalized with AT8+ soma (Fig. 8Ba–c); it was largely absent from AT8+ neuritic processes within plaques (Fig. 8Bd–f). Phosphorylated serine 178 (pS178) paxillin immunoreactivity was similarly detected in neuronal somata and nuclei throughout the hippocampi of control subjects; it was absent from the nuclei and was located in GVD bodies in AD (Fig. 9A). pS178 paxillin was observed in neuronal processes, GVD bodies and NFTs but not AT8+ neuritic threads (Fig. 9B).

Finally, we examined whether Hic-5 and paxillin are associated with phosphorylated tau (pTau) using a co-immunoprecipitation assay. pTau was contained within immunoprecipitates of Hic-5, paxillin or activated isoforms of paxillin (i.e. pY31, pY118) in AD but not control subjects (Fig. 10). Thus, Hic-5, paxillin and at least 2 phosphorylated isoforms of paxillin are stably associated with pTau in AD brain.

DISCUSSION

We postulated that the focal adhesion proteins paxillin and Hic-5 (which regulate integrin signaling in AD) may exhibit altered activation and subcellular distribution and that this might modulate neuronal function and contribute to its pathogenesis. Immunoblot analysis demonstrated Hic-5 and paxillin expression in human hippocampus, but failed to show significant alterations in detergent extracts from whole tissue; however, there were reduced Hic-5 levels in membrane fractions in Braak II-III AD subjects. By IHC, Hic-5 was predominately expressed in neurons within hippocampi and localized to NFTs in AD. Paxillin was detected in reactive astrocytes and CA1 pyramidal neurons, whereas phosphorylated isoforms of paxillin were observed in pyramidal neurons and NFTs throughout the AD hippocampi. Activated paxillin was also detected in NFTs and GVD bodies in AD hippocampi. These data suggest that the scaffolding proteins which link various intracellular signaling pathways to the ECM are altered in AD, possibly early in the disease.

Our data provide the first characterization of Hic-5 and paxillin expression and distribution in the human brain. Hic-5 is expressed predominantly in pyramidal neurons of human hippocampus. To date, the only known function of Hic-5 in neurons is its regulation of surface levels of DAT in rat midbrain neuronal cultures and inhibition of dopamine uptake (39). Within the midbrain a direct interaction between Hic-5 and DAT might be responsible for this effect. Our observation that Hic-5 protein levels are significantly elevated within the cytoplasm of CA1 pyramidal neurons in AD suggests that it may function similarly in sequestering cell surface receptors or transporters away from the plasma membrane to alter function and intracellular signaling. A recent study analyzed the expression and localization of dopamine receptor (DR1–5) subtypes in control vs. AD brain indicating that the dopaminergic system is altered in AD (52). Whether Hic-5 plays any role in regulating these dopamine receptor subtypes or other neuronal cell surface receptors during AD is not known at present.

Hic-5 was predominantly located within the cell body of pyramidal neurons and excluded from the nucleus in most cells in both control and AD hippocampi. Hic-5 was observed in the nuclei of a subset of CA1 pyramidal neurons and non-neuronal cells in AD subjects and it colocalized with pTau in NFTs. Hic-5 was also observed in the core of many amyloid plaques. Both oxidative stress and TGFβ are known regulators of Hic-5 expression and subcellular distribution but further studies are required to determine the potential role of oxidative stress in modulating Hic-5 distribution in the brain.

Paxillin was observed to be expressed predominantly in activated astrocytes throughout the hippocampi and elevated in AD subjects. Previous studies have not detected paxillin in astrocytes but rodent models of brain trauma exhibit increased paxillin only in reactive glia of the white matter, suggesting that initial glial reactions to trauma generate new “focal contacts” requiring GFAP and paxillin (53). Thus, it is possible that colocalization of paxillin in GFAP+ astrocytes reflects the generation of new focal adhesions required for astrocytic motility and activation in AD. Interestingly, paxillin was detected in focal granules in the nucleus of both CA1 pyramidal neurons and cells of the choroid plexus in

controls whereas paxillin immunoreactivity in the nucleus was decreased in AD subjects. While alterations in CA1 pyramidal neurons have been extensively observed in various neurodegenerative disorders and trauma, only more recent studies have observed alterations in the structure and function of the choroid plexus in AD (54–58). The choroid plexus is known to undergo morphological alterations in late stage AD (55, 56) and it has also been postulated that it may be responsible for removing Aβ from the cerebrospinal fluid (59). Changes in the localization of paxillin out of focal nuclear granules and the nucleus in both CA1 neurons and choroid plexus cells might reflect activation of key regulatory signaling pathways in AD.

Paxillin is phosphorylated on tyrosine residues Y31 and Y118 sites upon the initial activation of ECM-integrin signaling and the formation of intracellular focal adhesion sites. In cultured neurons, paxillin is also rapidly phosphorylated on tyrosine residues in the presence of fibrillar β-amyloid (1). Phosphorylation of paxillin on serine residues S126 and S178 is regulated by JNK signaling pathways (29–31, 60). We observed all phosphorylated isoforms of paxillin in the nucleus, soma and processes of pyramidal neurons in control subjects whereas the nuclear localization of all phosphorylated paxillin examined was reduced in AD. pY31 was rarely detected in NFTs, but pY118 was detected not only in NTS but also in GVD bodies with the soma of pyramidal neurons. The differences in staining of these 2 phosphorylated paxillin isoforms may reflect activation of distinct signaling pathways in AD. Both pS126 and pS178 were present in GVDs and NFTs in AD hippocampus, with highest levels in CA1. These results suggest that paxillin phosphorylation occurs during AD and that paxillin protein is re-distributed to intracellular protein aggregates and NFTs upon phosphorylation. We also noted the presence of phosphorylated paxillin in nuclei of non-neuronal cells.

We demonstrated an association between Hic-5, paxillin, pY31 and pY118 paxillin with phosphorylated tau in AD brains by co-immunoprecipitation assays using tissue lysates. These results suggest that paxillin and Hic-5 may modulate tau phosphorylation or associate with hyperphosphorylated tau in vivo. Further studies are required to determine whether the interactions between Hic-5, paxillin and tau occur prior to the formation of cytoplasmic aggregates or result only after the accumulation of proteins within aggregates and tangles. Our data suggest that altered Hic-5 and paxillin distribution in AD hippocampi occurred concurrent with tau and amyloid pathology but not prior to the accumulation of typical AD neuropathology. Biochemical data supporting direct interactions of pS126 and pS178 paxillin with tau awaits future studies.

The localization of phosphorylated paxillin within nuclei is a novel finding that warrants further investigation. Interestingly, there was decreased paxillin in CA1 pyramidal neuron nuclei and in choroid plexus cells in AD. The role of paxillin in the nucleus is poorly understood although it can function as a co-activator of gene expression and can bind poly(A) binding proteins to facilitate mRNA transport from the nucleus (35, 37). It is possible that phosphorylated paxillin may also regulate gene expression or mRNA trafficking in the hippocampus.

We note that antibodies to non-phosphorylated paxillin predominantly detected glial cells while antibodies to activated isoforms of paxillin predominantly labeled neurons and nuclei of non-neuronal cells. The basis for this difference may reflect the differential state of paxillin phosphorylation in neurons and glia. Prior in vitro models demonstrated that activation of astrocytes generated a loss of paxillin phosphorylation on tyrosine residues (61). This may result in the loss of immunoreactivity to activated astrocytes with antibodies to phosphorylated forms of paxillin.

In summary, our results provide novel insights into the distribution and activation state of focal adhesion proteins in AD, suggesting that altered signals from the ECM may modulate neuronal function, motility and survival in neurodegenerative diseases. Future studies will examine the functional role of these focal adhesion proteins in β-amyloid induced cell death as well as potential therapeutic targets for AD, and determine the function of Hic-5 and paxillin within neuronal nuclei.

Supplementary Material

Refer to Web version on PubMed Central for supplementary material.

ACKNOWLEDGMENTS

We thank Jonette Werley and Wanda Wang for expert technical assistance.

This work was supported by NIH NS042724 to RB.

REFERENCES

1. Grace EA, Busciglio J. Aberrant activation of focal adhesion proteins mediates fibrillar amyloid beta-induced neuronal dystrophy. J Neurosci. 2003; 23:493–502. [PubMed: 12533609]
2. Caltagarone J, Jing Z, Bowser R. Focal adhesions regulate Abeta signaling and cell death in Alzheimer's disease. Biochim Biophys Acta. 2007; 1772:438–445. [PubMed: 17215111]
3. Williamson R, Scales T, Clark BR, et al. Rapid tyrosine phosphorylation of neuronal proteins including tau and focal adhesion kinase in response to amyloid-beta peptide exposure: involvement of Src family protein kinases. J Neurosci. 2002; 22:10–20. [PubMed: 11756483]
4. Berg MM, Krafft GA, Klein WL. Rapid impact of beta-amyloid on paxillin in a neural cell line. J Neurosci Res. 1997; 50:979–989. [PubMed: 9452012]
5. Zhang C, Lambert MP, Bunch C, et al. Focal adhesion kinase expressed by nerve cell lines shows increased tyrosine phosphorylation in response to Alzheimer's A beta peptide. J Biol Chem. 1994; 269:25247–25250. [PubMed: 7929215]
6. Kontaxis, G.; Bister, K.; Konrat, R. LIM domain proteins. In: Messerschmidt, A., editor. Handbook of Metalloproteins. Chichester, UK: John Wiley & Sons; 2004. p. 378-389.
7. Howe A, Aplin AE, Alahari SK, et al. Integrin signaling and cell growth control. Curr Opin Cell Biol. 1998; 10:220–231. [PubMed: 9561846]
8. Giancotti FG, Ruoslahti E. Integrin signaling. Science. 1999; 285:1028–1032. [PubMed: 10446041]
9. Wehrle-Haller B, Imhof B. The inner lives of focal adhesions. Trends Cell Biol. 2002; 12:382–389. [PubMed: 12191915]
10. Aplin AE. Cell adhesion molecule regulation of nucleocytoplasmic trafficking. FEBS Lett. 2003; 534:11–14. [PubMed: 12527355]
11. Cary LA, Guan JL. Focal adhesion kinase in integrin-mediated signaling. Front Biosci. 1999; 4:D102–D113. [PubMed: 9889179]

12. Cordes N, Meineke V. Integrin signalling and the cellular response to ionizing radiation. J Mol Histol. 2004; 35:327–337. [PubMed: 15339052]
13. Guan JL. Focal adhesion kinase in integrin signaling. Matrix Biol. 1997; 16:195–200. [PubMed: 9402009]
14. Kornberg L, Earp HS, Parsons JT, et al. Cell adhesion or integrin clustering increases phosphorylation of a focal adhesion-associated tyrosine kinase. J Biol Chem. 1992; 267:23439–23442. [PubMed: 1429685]
15. Brown MC, Turner CE. Paxillin: Adapting to change. Physiol Rev. 2004; 84:1315–1339. [PubMed: 15383653]
16. Kadrmas JL, Beckerle MC. The LIM domain: From the cytoskeleton to the nucleus. Nat Rev Mol Cell Biol. 2004; 5:920–931. [PubMed: 15520811]
17. Nishiya N, Tachibana K, Shibanuma M, et al. Hic-5-reduced cell spreading on fibronectin: competitive effects between paxillin and Hic-5 through interaction with focal adhesion kinase. Mol Cell Biol. 2001; 21:5332–5345. [PubMed: 11463817]
18. Shibanuma M, Kim-Kaneyama JR, Ishino K, et al. Hic-5 communicates between focal adhesions and the nucleus through oxidant-sensitive nuclear export signal. Mol Biol Cell. 2003; 14:1158–1171. [PubMed: 12631731]
19. Schroeder MJ, Webb DJ, Shabanowitz J, et al. Methods for the detection of paxillin post-translational modifications and interacting proteins by mass spectrometry. J Proteome Res. 2005; 4:1832–1841. [PubMed: 16212439]
20. Webb DJ, Schroeder MJ, Brame CJ, et al. Paxillin phosphorylation sites mapped by mass spectrometry. J Cell Sci. 2005; 118:4925–4929. [PubMed: 16254239]
21. Shibanuma M, Mochizuki E, Maniwa R, et al. Induction of senescence-like phenotypes by forced expression of hic-5, which encodes a novel LIM motif protein, in immortalized human fibroblasts. Mol Cell Biol. 1997; 17:1224–1235. [PubMed: 9032249]
22. Thomas SM, Hagel M, Turner CE. Characterization of a focal adhesion protein, Hic-5, that shares extensive homology with paxillin. J Cell Sci. 1999; 112:181–190. [PubMed: 9858471]
23. Gao Z, Schwartz LM. Identification and analysis of Hic-5/ARA55 isoforms: Implications for integrin signaling and steroid hormone action. FEBS Lett. 2005; 579:5651–5657. [PubMed: 16219310]
24. Gao ZL, Deblis R, Glenn H, et al. Differential roles of HIC-5 isoforms in the regulation of cell death and myotube formation during myogenesis. Exp Cell Res. 2007:4000–4014. [PubMed: 17935713]
25. de Curtis I, Malanchini B. Integrin-mediated tyrosine phosphorylation and redistribution of paxillin during neuronal adhesion. Exp Cell Res. 1997; 230:233–243. [PubMed: 9024782]
26. Leventhal PS, Feldman EL. Tyrosine phosphorylation and enhanced expression of paxillin during neuronal differentiation in vitro. J Biol Chem. 1996; 271:5957–5960. [PubMed: 8626373]
27. Schaller MD, Parsons JT. pp125FAK-dependent tyrosine phosphorylation of paxillin creates a high-affinity binding site for Crk. Mol Cell Biol. 1995; 15:2635–2645. [PubMed: 7537852]
28. Turner CE, Schaller M, Parsons JT. Tyrosine phosphorylation of the focal adhesion kinase pp125FAK during development: Relation to paxillin. J Cell Sci. 1993; 105:637–645. [PubMed: 8408291]
29. Huang C, Borchers CH, Schaller MD, et al. Phosphorylation of paxillin by p38MAPK is involved in the neurite extension of PC-12 cells. J Cell Biol. 2004; 164:593–602. [PubMed: 14970194]
30. Huang C, Jacobson K, Schaller MD. A role for JNK-paxillin signaling in cell migration. Cell Cycle. 2004; 3:4–6. [PubMed: 14657652]
31. Huang C, Rajfur Z, Borchers C, et al. JNK phosphorylates paxillin and regulates cell migration. Nature. 2003; 424:219–223. [PubMed: 12853963]
32. Ghogomu SM, van Venrooy S, Ritthaler M, et al. HIC-5 is a novel repressor of lymphoid enhancer factor/T-cell factor-driven transcription. J Biol Chem. 2006; 281:1755–1764. [PubMed: 16291758]
33. Guerrero-Santoro J, Yang L, Stallcup MR, et al. Distinct LIM domains of Hic-5/ARA55 are required for nuclear matrix targeting and glucocorticoid receptor binding and coactivation. J Cell Biochem. 2004; 92:810–819. [PubMed: 15211577]

34. Heitzer MD, DeFranco DB. Mechanism of action of Hic-5/androgen receptor activator 55, a LIM domain-containing nuclear receptor coactivator. Mol Endocrinol. 2006; 20:56–64. [PubMed: 16141357]
35. Kasai M, Guerrero-Santoro J, Friedman R, et al. The Group 3 LIM domain protein paxillin potentiates androgen receptor transactivation in prostate cancer cell lines. Cancer Res. 2003; 63:4927–4935. [PubMed: 12941817]
36. Shibanuma M, Kim-Kaneyama JR, Sato S, et al. A LIM protein, Hic-5, functions as a potential coactivator for Sp1. J Cell Biochem. 2004; 91:633–645. [PubMed: 14755691]
37. Woods AJ, Roberts MS, Choudhary J, et al. Paxillin associates with poly(A)-binding protein 1 at the dense endoplasmic reticulum and the leading edge of migrating cells. J Biol Chem. 2002; 277:6428–6437. [PubMed: 11704675]
38. Yang L, Guerrero J, Hong H, et al. Interaction of the tau2 transcriptional activation domain of glucocorticoid receptor with a novel steroid receptor coactivator, Hic-5, which localizes to both focal adhesions and the nuclear matrix. Mol Biol Cell. 2000; 11:2007–2018. [PubMed: 10848625]
39. Carneiro AM, Ingram SL, Beaulieu JM, et al. The multiple LIM domain-containing adaptor protein Hic-5 synaptically colocalizes and interacts with the dopamine transporter. J Neurosci. 2002; 22:7045–7054. [PubMed: 12177201]
40. Angers-Loustau A, Cote JF, Charest A, et al. Protein tyrosine phosphatase-PEST regulates focal adhesion disassembly, migration, and cytokinesis in fibroblasts. J Cell Biol. 1999; 144:1019–1031. [PubMed: 10085298]
41. Braak H, Braak E. Neuropathological stageing of Alzheimer-related changes. Acta Neuropathol (Berl). 1991; 82:239–259. [PubMed: 1759558]
42. Shaw LM, Korecka M, Clark CM, et al. Biomarkers of neurodegeneration for diagnosis and monitoring therapeutics. Nat Rev Drug Discov. 2007; 6:295–303. [PubMed: 17347655]
43. Wilkinson BL, Landreth GE. The microglial NADPH oxidase complex as a source of oxidative stress in Alzheimer's disease. J Neuroinflammation. 2006; 3:30. [PubMed: 17094809]
44. Hyman BT, Trojanowski JQ. Consensus recommendations for the postmortem diagnosis of Alzheimer disease from the National Institute on Aging and the Reagan Institute Working Group on diagnostic criteria for the neuropathological assessment of Alzheimer disease. J Neuropathol Exp Neurol. 1997; 56:1095–1097. [PubMed: 9329452]
45. Michelsen JW, Schmeichel KL, Beckerle MC, et al. The LIM motif defines a specific zinc-binding protein domain. Proc Natl Acad Sci U S A. 1993; 90:4404–4408. [PubMed: 8506279]
46. Mirra SS, Heyman A, McKeel D, et al. The Consortium to Establish a Registry for Alzheimer's Disease (CERAD). Part II. Standardization of the neuropathologic assessment of Alzheimer's disease. Neurology. 1991; 41:479–486. [PubMed: 2011243]
47. Morris JC, Heyman A, Mohs RC, et al. The Consortium to Establish a Registry for Alzheimer's Disease (CERAD). Part I. Standardization of the neuropathologic assessment of Alzheimer's disease. Neurology. 1989; 39:1159–1165. [PubMed: 2771064]
48. Caltagarone J, Rhodes J, Honer WG, et al. Localization of a novel septin protein, hCDCrel-1, in neurons of human brain. Neuroreport. 1998; 9:2907–2912. [PubMed: 9760144]
49. Holland T. The comparative power of the discriminant methods used in toxicological pathology. Toxicol Pathol. 2005; 33:490–494. [PubMed: 16036867]
50. Young BA, Taooka Y, Liu S, et al. The cytoplasmic domain of the integrin alpha9 subunit requires the adaptor protein paxillin to inhibit cell spreading but promotes cell migration in a paxillin-independent manner. Mol Biol Cell. 2001; 12:3214–3225. [PubMed: 11598204]
51. Heitzer MD, DeFranco DB. Hic-5/ARA55, a LIM domain-containing nuclear receptor coactivator expressed in prostate stromal cells. Cancer Res. 2006; 66:7326–7333. [PubMed: 16849583]
52. Kumar U, Patel SC. Immunohistochemical localization of dopamine receptor subtypes (D1R–D5R) in Alzheimer's disease brain. Brain Res. 2007; 1131:187–196. [PubMed: 17182012]
53. Kalman M, Szabo A. Immunohistochemical investigation of actin-anchoring proteins vinculin, talin and paxillin in rat brain following lesion: A moderate reaction, confined to the astroglia of brain tracts. Exp Brain Res. 2001; 139:426–434. [PubMed: 11534866]
54. Johanson C, McMillan P, Tavares R, et al. Homeostatic capabilities of the choroid plexus epithelium in Alzheimer's disease. Cerebrospinal Fluid Res. 2004; 1:1–16. [PubMed: 15679934]

55. Serot JM, Bene MC, Foliguet B, et al. Altered choroid plexus basement membrane and epithelium in late-onset Alzheimer's disease: an ultrastructural study. Ann N Y Acad Sci. 1997; 826:507–509. [PubMed: 9329734]

56. Serot JM, Bene MC, Foliguet B, et al. Morphological alterations of the choroid plexus in late-onset Alzheimer's disease. Acta Neuropathol (Berl). 2000; 99:105–108. [PubMed: 10672315]

57. Silverberg G, Mayo M, Saul T, et al. Elevated cerebrospinal fluid pressure in patients with Alzheimer's disease. Cerebrospinal Fluid Res. 2006; 3:1–6. [PubMed: 16390539]

58. Silverberg GD, Heit G, Huhn S, et al. The cerebrospinal fluid production rate is reduced in dementia of the Alzheimer's type. Neurology. 2001; 57:1763–1766. [PubMed: 11723260]

59. Crossgrove JS, Li GJ, Zheng W. The choroid plexus removes beta-amyloid from brain cerebrospinal fluid. Exp Biol Med (Maywood). 2005; 230:771–776. [PubMed: 16246905]

60. Abou, Zeid N.; Valles, AM.; Boyer, B. Serine phosphorylation regulates paxillin turnover during cell migration. Cell Commun Signal. 2006; 4:1–12. [PubMed: 16403231]

61. Padmanabhan J, Clayton D, Shelanski ML. Dibutyryl cyclic AMP-induced process formation in astrocytes is associated with a decrease in tyrosine phosphorylation of focal adhesion kinase and paxillin. J Neurobiol. 1999; 39:407–422. [PubMed: 10363913]

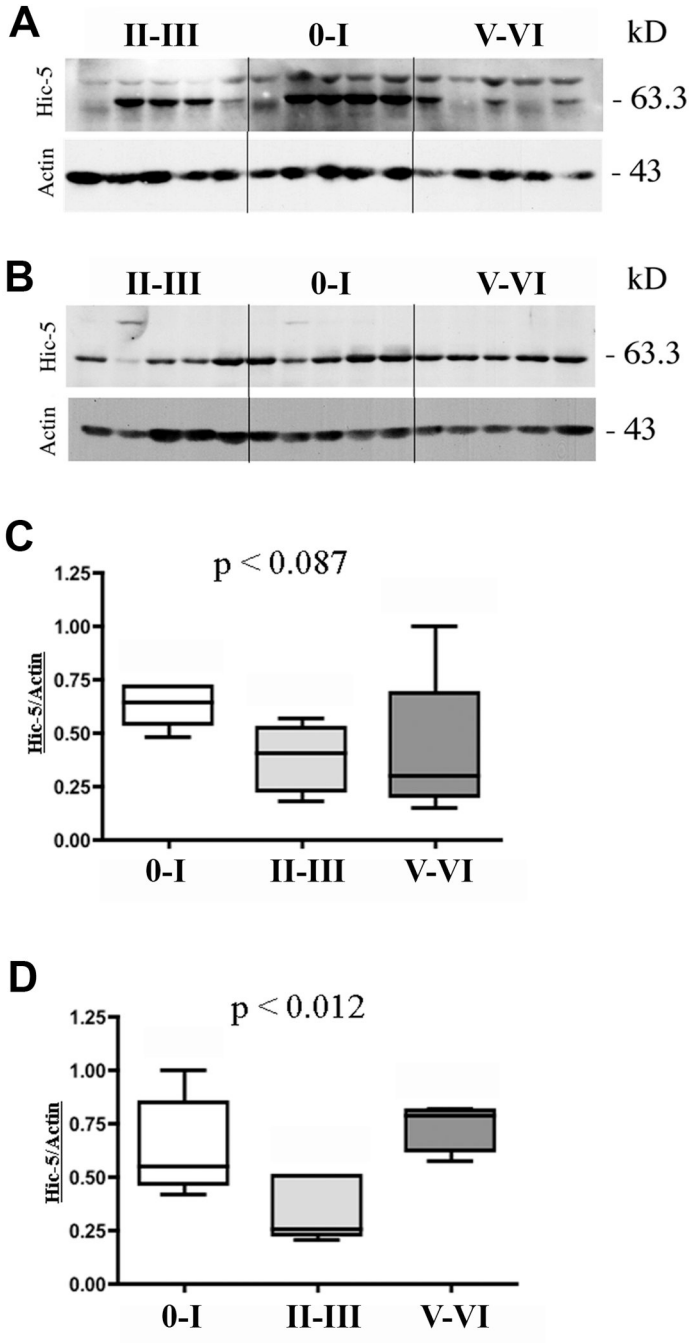

Figure 1.

Immunoblot analysis for Hic-5 protein in TX-100-soluble and -insoluble fractions Fresh frozen hippocampi from 5 non-neurologic disease controls and 10 Alzheimer disease (AD) subjects were homogenized to generate TX-100-soluble (**A**) and -insoluble (**B**) fractions. Equal amounts of protein were loaded in gel lanes and Braak stages are indicated above the lanes. Antibody to actin was used as a loading control. Lanes 1 to 5 are from early-stage AD, lanes 6 to 10 are from control subjects and lanes 11 to 15 are from late-stage AD subjects. Quantitative measurements for each lane were normalized to actin and the highest

value was arbitrarily set to 1. Hippocampal Hic-5 protein levels across the 3 Braak stage groups in TX-100-soluble fraction (**C**) and -insoluble (**D**) fractions are shown. **C**, $p < 0.087$; **D**, $p < 0.012$ for Braak stage II-III.

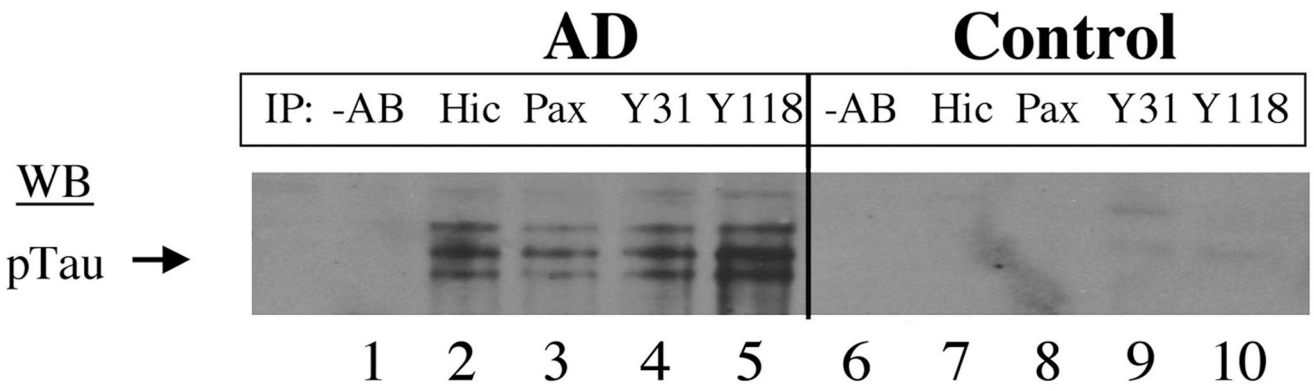

Figure 2.

Hic-5 localization and relative expression in the CA3 and CA1 subfields (**A**) Hic-5 immunoreactivity in CA3 pyramidal neurons in control and AD subjects (**a–c**). Hic-5 immunoreactivity in CA1 pyramidal neurons in control and AD subjects (**d–f**). Scale bar = 50 μm for all panels. (**B**) Mann-Whitney test comparing Hic-5 immunoreactivity in control vs. AD subjects. (**C**) Kruskal-Wallis test comparing Hic-5 immunoreactivity across all 3 Braak stage groups.

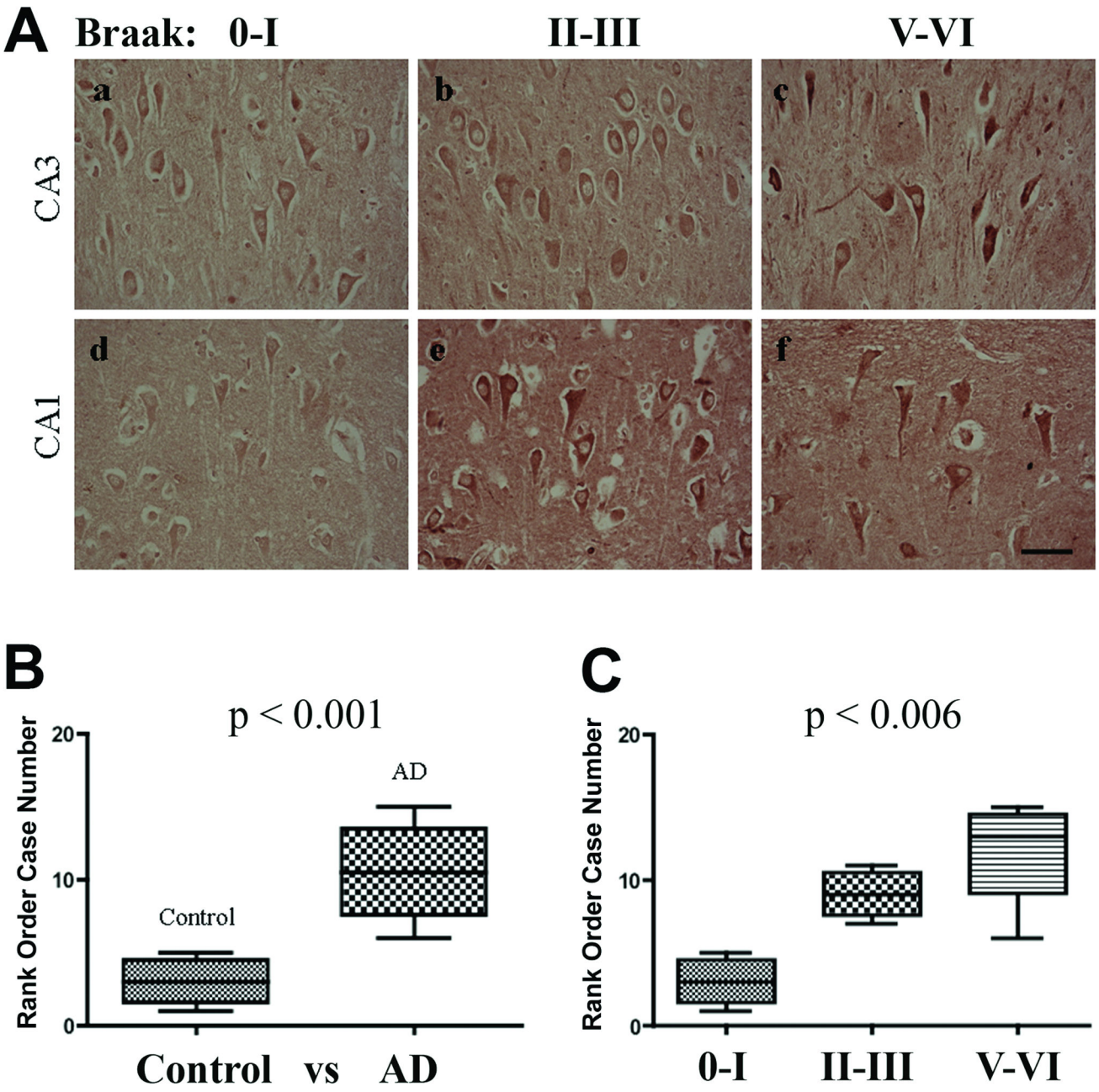

Figure 3.

Hic-5 distribution in Alzheimer disease (AD) hippocampi. Confocal microscopy with Hic-5 (green), nuclei (blue) and β-amyloid, pTau (AT8), or microglia (CD68) (red). Hic-5 was localized to pyramidal neurons, their processes and cores within β-amyloid+ plaques (**a–c**). Arrow in (**a**) indicates a beaded process that projects through the plaque in (**c**). Hic-5 was not contained in neuritic plaque components labeled by AT8 (**d–f**) but a subset of AT8+ neurofibrillary tangles (NFTs) within pyramidal neurons contain Hic-5 (**d–i**). Arrow in (**g**)

indicates Hic-5 in a pyramidal neuron that lacks NFTs (**g–i**). Hic-5 was also located in nuclei of CD68+ microglia within plaques (**j–l**). Scale bars = 50 μm for all panels.

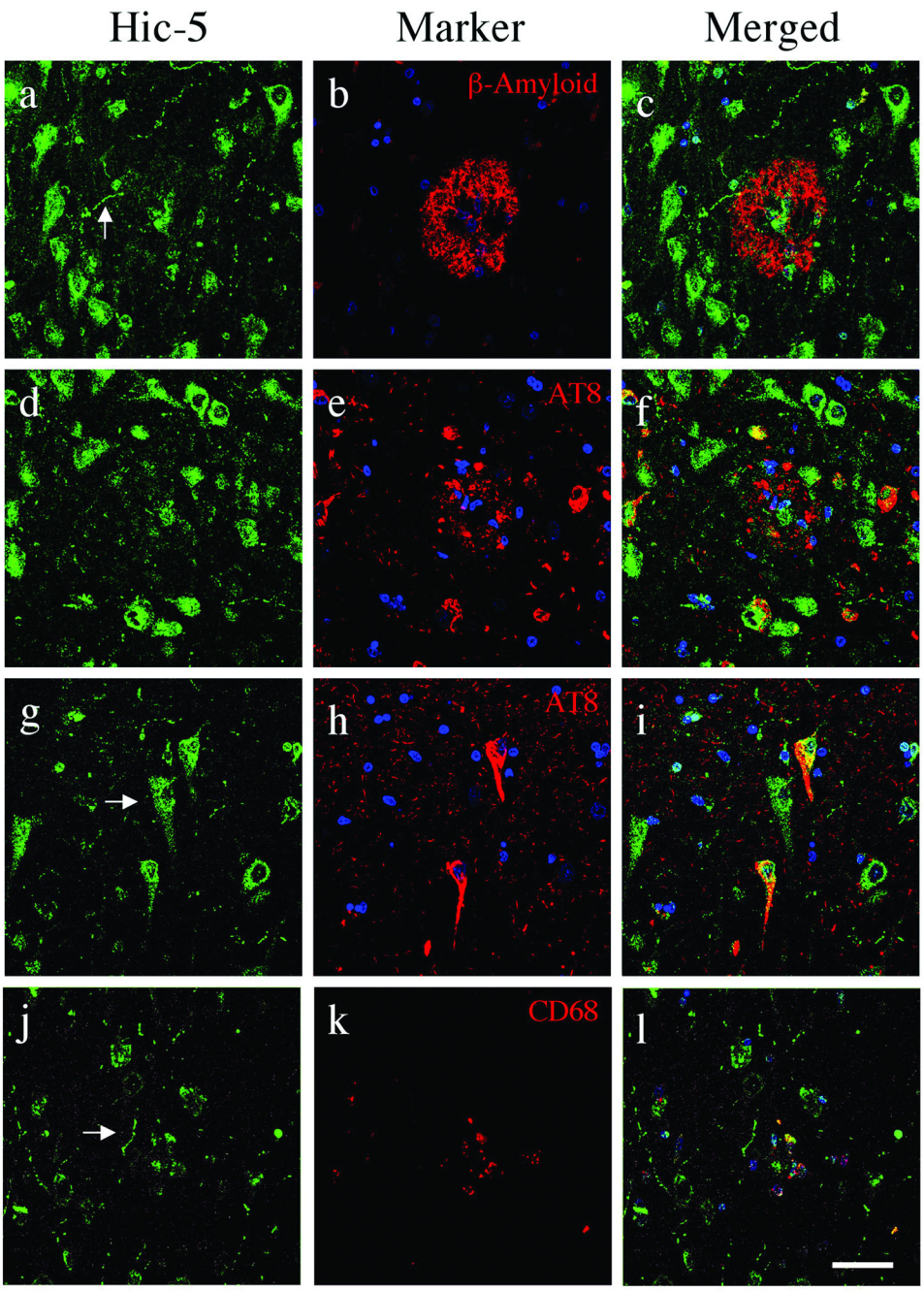

Figure 4.

Paxillin expression in control and Alzheimer disease (AD) hippocampi. (**A**) Low-power magnification reveals paxillin immunoreactivity in the alveus/white matter (WM) tracts and the stratum lacunosum (SL) layer in both control (**a**) and AD (**b**) subjects. In the hilus/CA4 of control subjects, paxillin is localized to reactive astrocytes and neuropil (**c**). AD hippocampus exhibits elevated paxillin immunoreactivity in reactive astrocytes throughout the hippocampus and within plaques (**d**). Higher power magnification of CA1 pyramidal neurons reveals punctate nuclear paxillin distribution in control (**e**) but not AD (**f**). Scale

bars: **a, b** = 500 μm; **c** = 100 μm; **d** = 50 μm; **e, f** = 25 μm. (**B**) Mann Whitney statistical test comparing paxillin levels in control vs. AD subjects.

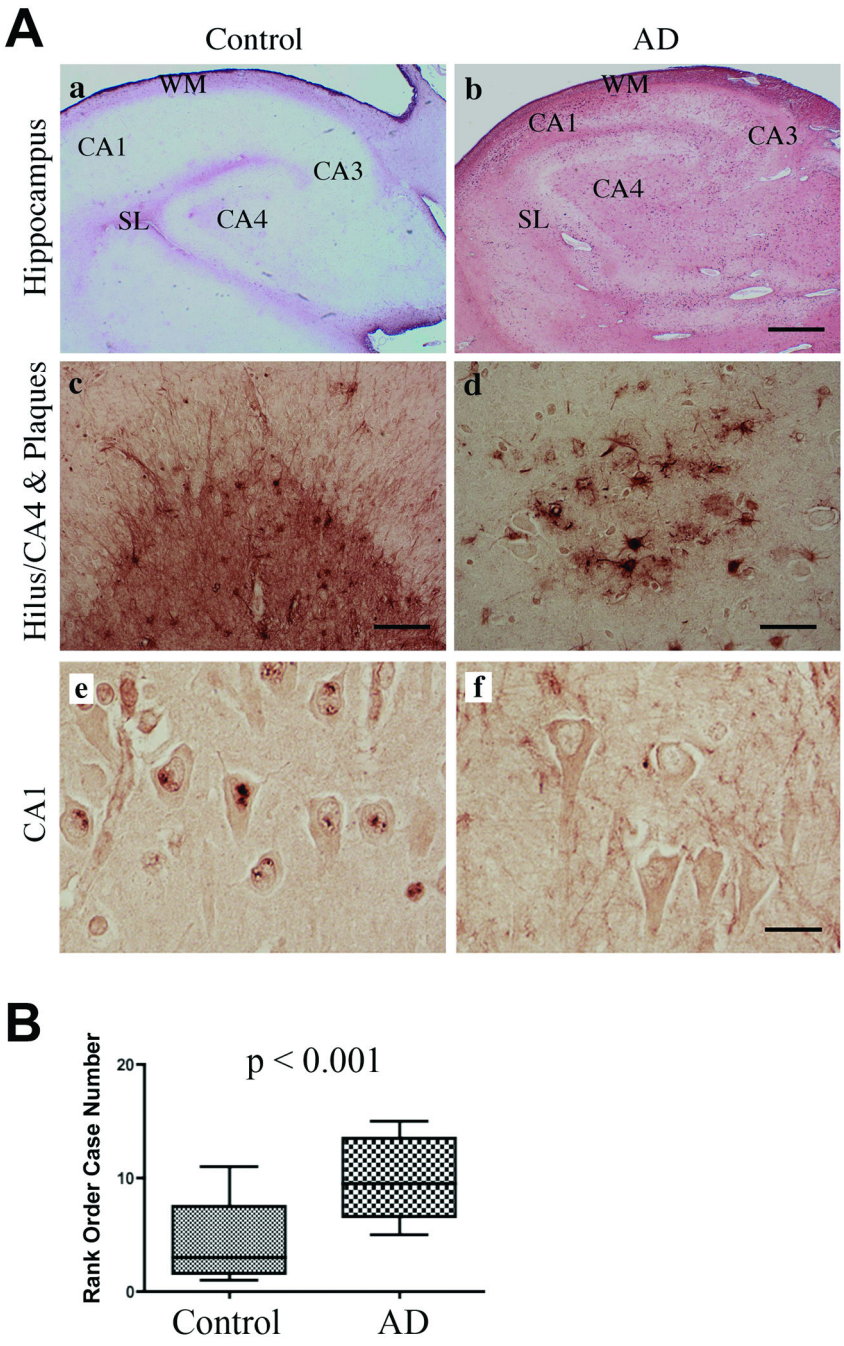

Figure 5.

Paxillin localization in Alzheimer disease (AD). Confocal microscopy of an AD hippocampus with paxillin (green), nuclei (blue) and β-amyloid, reactive astrocytes (glial fibrillary acidic protein [GFAP]), and pTau (AT8) (red). Paxillin is detected in reactive astrocytes and numerous processes that surround and penetrate β-amyloid+ plaques throughout the AD hippocampus (**a–c**). Paxillin immunofluorescence is observed in the majority of GFAP+ astrocytes surrounding plaques (**d–f**). Paxillin was not detected in AT8+ neurofibrillary tangles or nuclei (**g–i**). Scale bars = 50 μm for all panels.

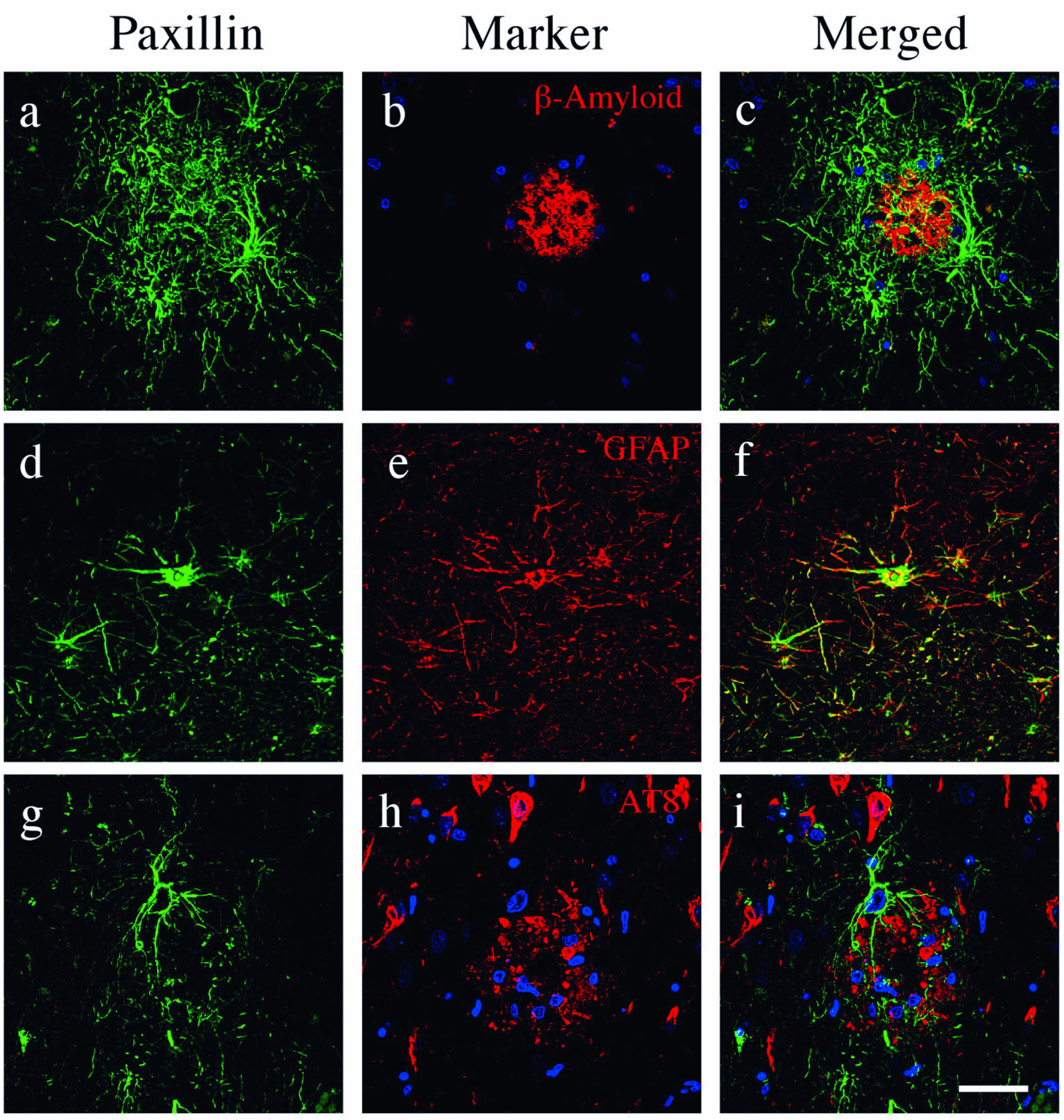

Figure 6.

Phosphorylated Y31 (pY31) paxillin in control and Alzheimer disease (AD) hippocampi. (**A**) pY31 paxillin is located in pyramidal neurons in control and AD hippocampi but with no nuclear staining in AD (**a, b**). pY31 paxillin is localized in Hirano bodies (HB) (**c**) and plaques (**d**). (**B**) Confocal microscopy for pY31 paxillin (green), nuclei (blue) and AT8-labeled phosphorylated Tau (pTau) (red). pY31 paxillin is colocalized in AT8+ pyramidal neurons in both neurofibrillary tangles and neuritic processes in AD (**a–f**). Scale bars: **A, B** = 50 μm.

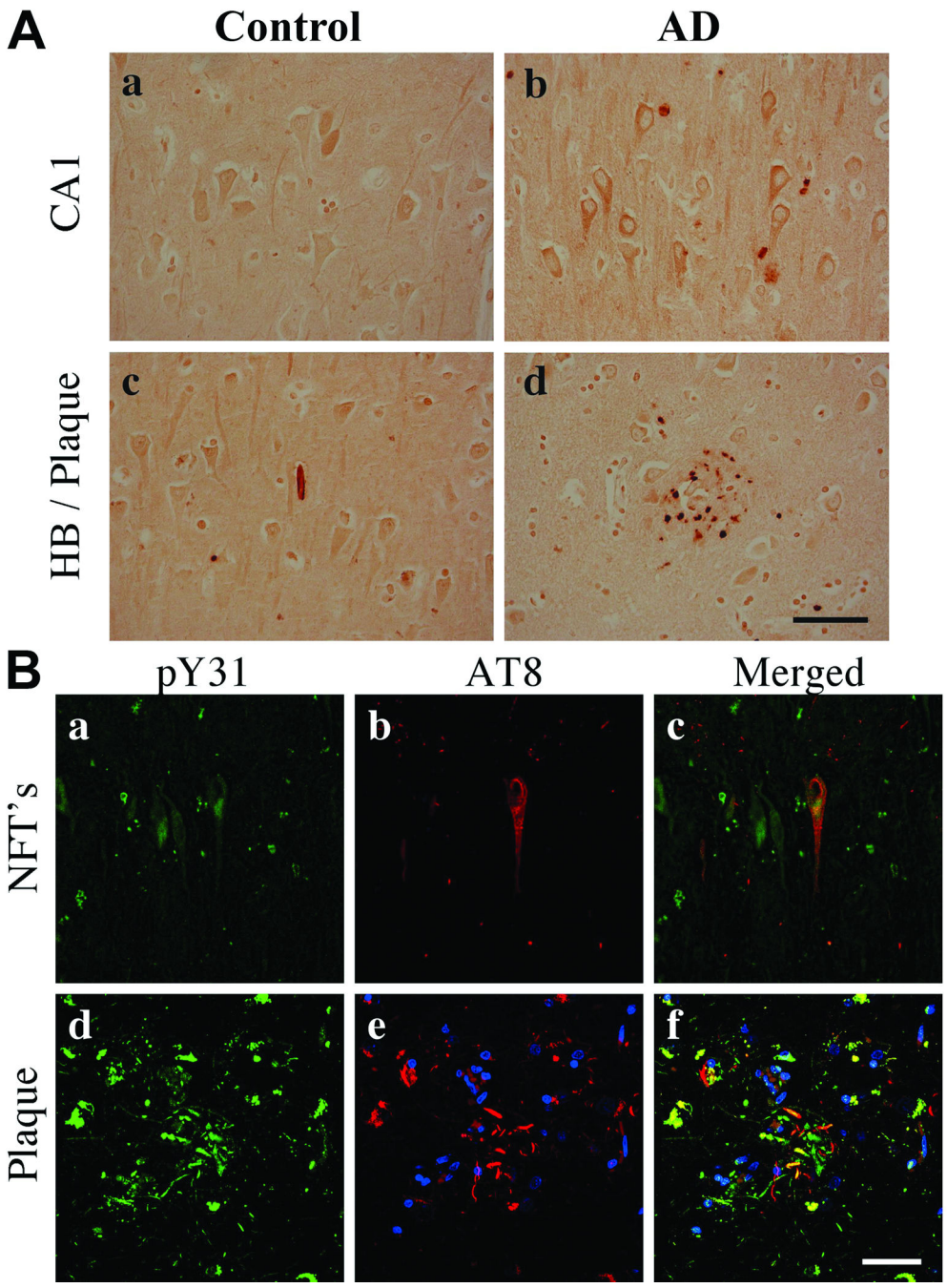

Figure 7.

Phosphorylated Y118 (pY118) paxillin in control and Alzheimer disease (AD) hippocampi. (**A**) CA1 pyramidal neurons exhibit nuclear pY118 in control and pY118 in granulovacuolar (GVD) bodies in AD. Insets are high power magnifications of CA1 pyramidal neurons. (**b**) Arrows in inset indicate GVD bodies. pY118 paxillin phospho-specific and nonspecific peptide blocking controls demonstrate antibody specificity (**c, d**). (**B**) Confocal microscopy for pY118 paxillin (green), nuclei (blue) and AT8 labeled phosphorylated Tau (pTau) (red). pY118 paxillin is colocalized in the majority of AT8+ pyramidal neurons in both

neurofibrillary tangles (NFTs) and processes within plaques (**a–f**). Note the extensive colocalization of pY118 paxillin in nuclei of neuronal and non-neuronal cells. Scale bars: **A** = 50 μm for **a** and **b**; 500 μm for **c** and **d**; **B** = 50 μm for all panels.

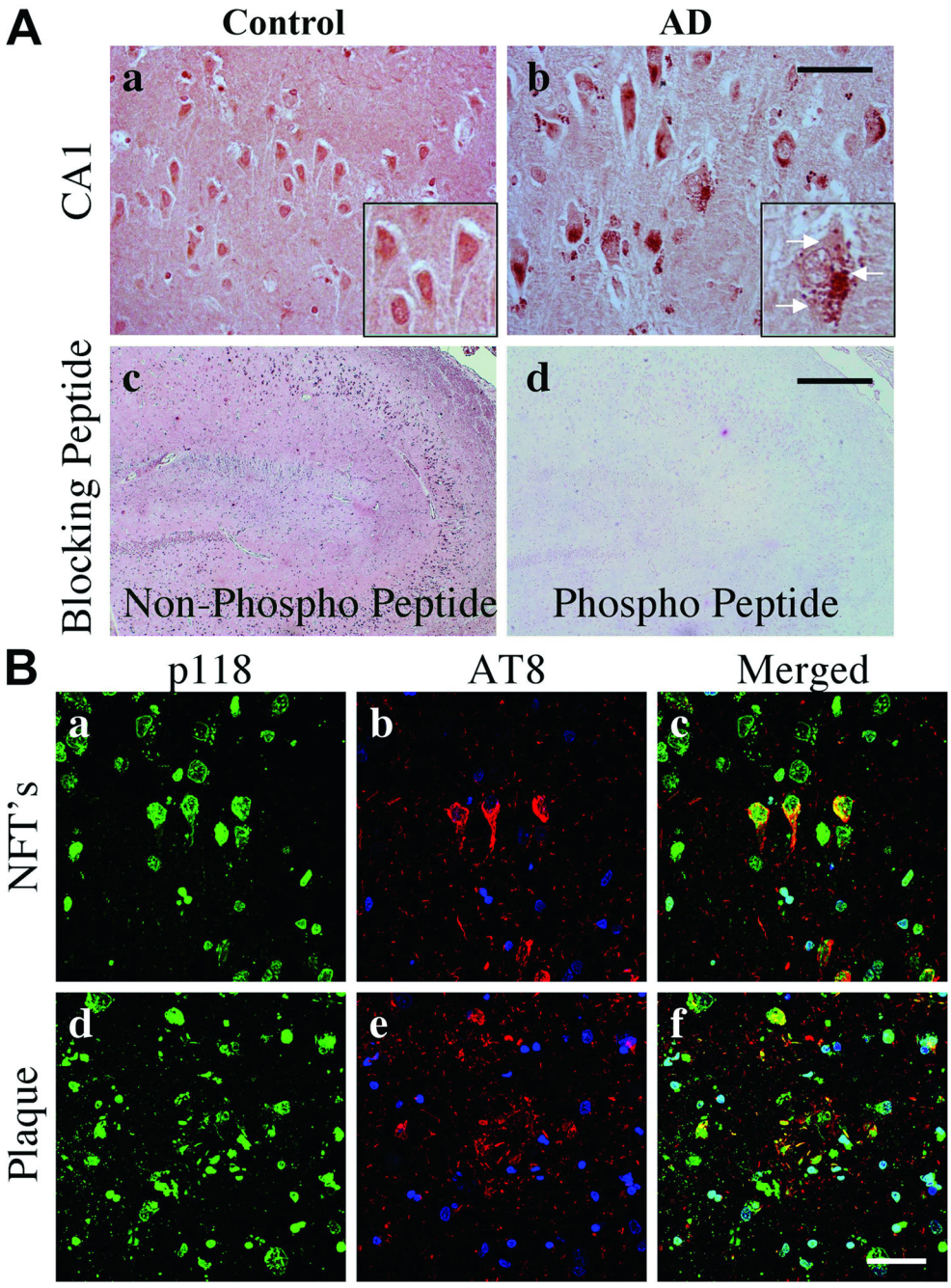

Figure 8.

Phosphorylated S126 (pS126) paxillin in control and Alzheimer disease (AD) hippocampi. (**A**) CA1 pyramidal neurons in AD hippocampus contain pS126 paxillin in granulovacuolar degeneration (GVD) bodies and reduced nuclear pS126 paxillin compared to controls. Insets are high power magnifications of pS126 paxillin in CA1 pyramidal neurons (**a, b**). pS126 paxillin phospho-specific and nonspecific peptide blocking controls demonstrate antibody specificity (**c, d**). (**B**) Confocal microscopy for pS126 paxillin (green), nuclei (blue) and AT8 labeled phosphorylated Tau (red). pS126 paxillin colocalized to AT8+ neurofibrillary

tangles (**a–f**). Scale bars: **A** = 50 μm for **a** and **b**; 500 μm for **c** and **d; B** = 50 μm for all panels.

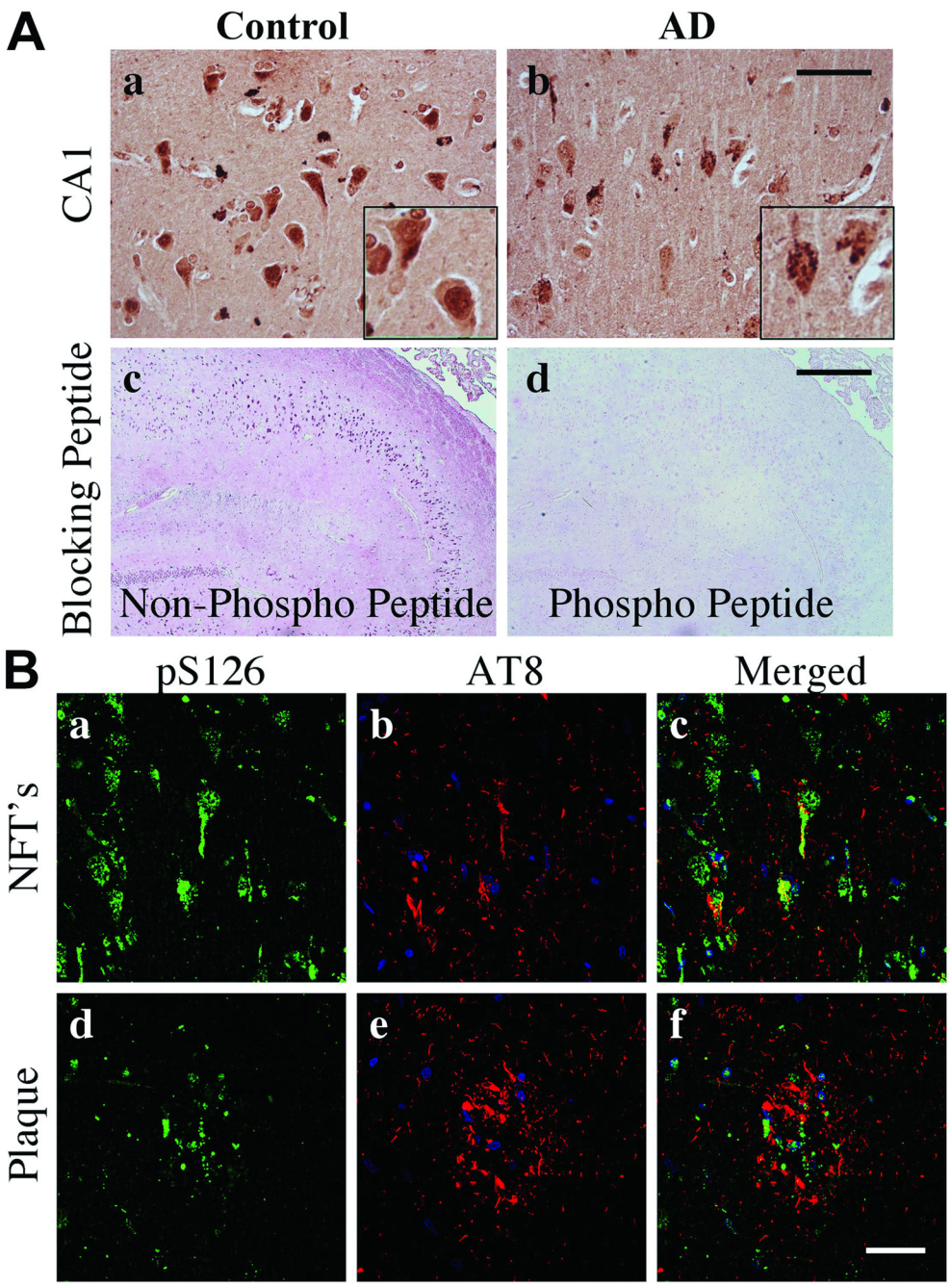

Figure 9.

Phosphorylated S178 (pS178) paxillin in the control and Alzheimer disease (AD) hippocampi. (**A**) pS178 paxillin in control and AD hippocampus. CA1 pyramidal neurons in AD hippocampus exhibit reduced pS178 paxillin in the nucleus and immunoreactivity in GVD bodies. Insets are high power magnification of pS178 paxillin immunoreactivity in CA1 pyramidal neurons. (**B**) Triple label confocal microscopy with pS178 paxillin (green), nucleus (blue) and AT8 labeled pTau (red). pS178 paxillin immunofluorescence colocalized in a majority of AT8 positive NFTs in pyramidal neurons. Scale bar: 50 μm for all panels.

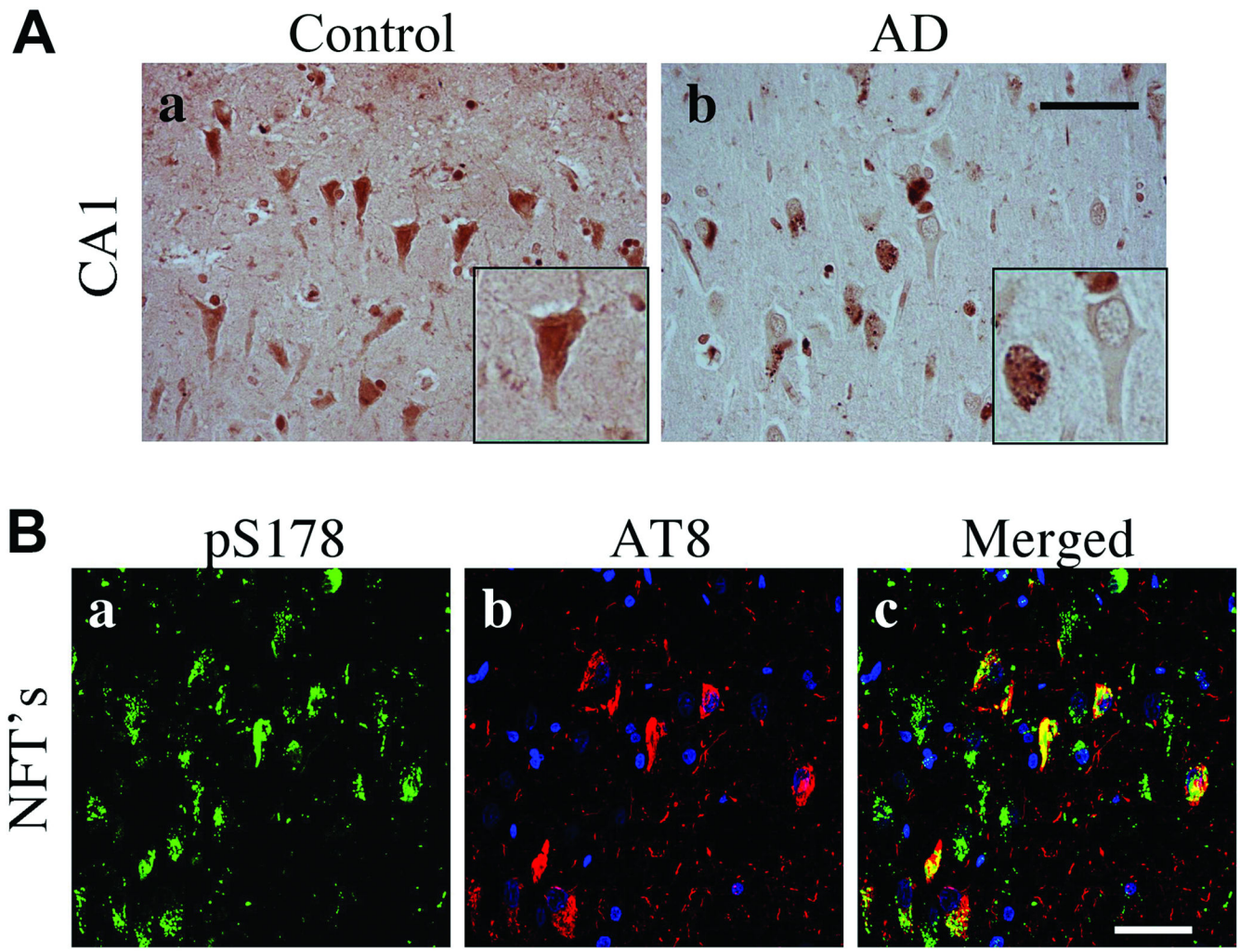

Figure 10.

Co-immunoprecipitation assays. Fresh frozen hippocampi from Alzheimer disease (AD) (lanes 1–5) and non-neurologic disease control (lanes 6–10) cases were used for immunoprecipitation studies. Equal amounts of protein from each total homogenate were immunoprecipitated (IP) with antibodies listed above each gel lane. Lanes 1 and 6 (–AB): no primary antibody control. Lanes 2 and 7 (Hic): Hic-5 antibody. Lanes 3 and 8 (Pax): paxillin. Lanes 4 and 9 (Y31): pY31 paxillin. Lanes 5 and 10 (Y118): pY118 paxillin. Eluted proteins were loaded in gel lanes and the resulting blot immunolabeled for phosphorylated tau (pTau) using AT8 antibody.

Table 1

Cases Studied

Case No.	Age (years)	Sex	Braak Stage	Brain Weight (grams)	Postmortem Interval (hours)
Controls					
1	51	F	0	1400	5
2	51	M	0	1310	6
3	57	M	I	1450	2
4	68	M	I	1380	27
5	70	F	0	1200	6
Alzheimer Disease					
6	56	F	II	1190	19
7	66	F	II	1160	9
8	71	M	II	1340	15
9	72	F	II	1120	9
10	76	M	III	1545	13
11	57	F	VI	900	9
12	58	M	VI	1250	7
13	69	F	V	960	5
14	70	M	VI	1240	3
15	71	F	VI	1030	4.5

Five control subjects had no tangle pathology (Braak stage 0 – I); 5 subjects had Braak stage II – III pathology; 5 subjects had Braak stage V – VI pathology (end-stage AD). F = female; M = male.

Table 2

Antibodies

Antibody/ Antigen	Host Species, Dilution	Source	Specificity*
Hic-5/ARA55	Rabbit 1:300	GenWay SanDiego, CA	Hic-5 cell adhesion redox sensitive
Paxillin	Rabbit 1:300	Epitomics Burlingame, CA	Paxillin, cell adhesion
pY31 Paxillin	Rabbit 1:300	Epitomics	Modification during FA formation
pY116 Paxillin	Rabbit 1:100	Biosource Camarillo, CA	Modification during FA formation by Crk/Src and FAK after integrin activation
pS126 Paxillin	Rabbit 1:100	Biosource	Modified after Raf stimulation in GSK3 pathway
pS178 Paxillin	Rabbit 1:100	Biosource	Modified by cdc2 kinase during mitosis, JNK during cell migration
β-Amyloid	Mouse 1:300	Dako Carpinteria, CA	Plaques
AT8	Mouse 1:300	Pierce Rockford, IL	Hyperphosphorylated tau
GFAP	Mouse 1:1000	Dako	Activated astrocytes
CD68	Mouse 1:100	Dako	Mature and immature Microglia
TO-PRO-3	1:300	Invitrogen Carlsbad, CA	Nuclei

*As reported on the company data information sheet. FA = focal adhesion.